Eur. Phys. J. A **16**, 549–561 (2003)
DOI 10.1140/epja/i2002-10131-8

THE EUROPEAN PHYSICAL JOURNAL A

Lifetime of heavy hypernuclei and its implications on the weak ΛN interaction

W. Cassing[1], L. Jarczyk[2], B. Kamys[2], P. Kulessa[3,4], H. Ohm[3], K. Pysz[3,4], Z. Rudy[2,3], O.W.B. Schult[3], and H. Ströher[3,a]

[1] Institut für Theoretische Physik, Justus Liebig Universität Giessen, D-35392 Giessen, Germany
[2] M. Smoluchowski Institute of Physics, Jagellonian University, PL-30059 Cracow, Poland
[3] Institut für Kernphysik, Forschungszentrum Jülich, D-52425 Jülich, Germany
[4] H. Niewodniczański Institute of Nuclear Physics, PL-31342 Cracow, Poland

Received: 8 August 2002 / Revised version: 20 December 2002 /
Published online: 25 March 2003 –
Communicated by Th. Walcher

Abstract. The lifetime of the Λ-hyperon in heavy hypernuclei measured in proton-Au, -Bi and -U collisions by the COSY-13 Collaboration at COSY-Jülich has been analyzed to yield $\tau_\Lambda = (145 \pm 11)$ ps. This value for τ_Λ is compatible with the lifetime extracted from antiproton annihilation on Bi and U targets, albeit much more accurate. Theoretical models based on the meson exchange picture and assuming the validity of the phenomenological $\Delta I = 1/2$ rule predict the lifetime of heavy hypernuclei to be significantly larger (2-3 standard deviations). Such large differences indicate that at least one of the assumptions in these models is not fulfilled. A much better reproduction of the lifetimes of heavy hypernuclei is achieved in the phase space model, if the $\Delta I = 1/2$ rule is discarded in the nonmesonic Λ decay.

PACS. 13.30.-a Decays of baryons – 13.75.Ev Hyperon-nucleon interactions – 21.80.+a Hypernuclei – 25.80.Pw Hyperon-induced reactions

1 Introduction

The Λ-hyperon decay can be studied for free hyperons as well as for hyperons colliding with nucleons inside the nuclear medium. In the first case it proceeds via the mesonic process, $\Lambda \to \pi + N$, with an energy release of about 38 MeV, whereas collisions with nucleons lead to the nonmesonic decay, *e.g.* $N+\Lambda \to N+N$, with an energy release of (~ 180 MeV).

The mesonic decay also occurs for hyperons bound in nuclei, but it is strongly inhibited for all but the lightest hypernuclei due to Pauli blocking of the nucleon final states. The nonmesonic decay, on the other hand, can be studied only in hypernuclei because neither Λ-hyperon beams nor targets are available. Due to the immense difficulty in producing Λ-hypernuclei and in subsequently detecting their decay the available experimental data on the nonmesonic process are scarce and have large uncertainties.

Most of the decay measurements of hypernuclei have been performed for small mass numbers and suffer from low statistics (see, *e.g.*, the reviews [1–3] or refs. [4–10]). Even the total decay rate (or inverse lifetime) of heavy hypernuclei was, up to very recently, known only with a large error [11]. The experimental knowledge of the partial decay rates is also not satisfactory, *e.g.* the experimental studies devoted to light ($A \leq 28$) [4–7,10] and medium heavy ($40 < A < 100$) hypernuclei [12–14] report different values for the neutron- and proton-induced decay rates (Γ_n and Γ_p). The results for Γ_n/Γ_p for light hypernuclei are close to unity, whereas those for heavy hypernuclei vary between 1.5 and 9.0. The experimental situation shows —together with uncertainties in the theoretical description— that the nonmesonic process is barely understood so far.

We recall that in the Standard Model the weak $|\Delta S| = 1$ transitions can proceed with both $\Delta I = 1/2$ and $\Delta I = 3/2$ amplitudes. However, it was found experimentally (in the decays of free kaons and hyperons) that the $\Delta I = 1/2$ amplitudes dominate by far the $|\Delta S| = 1$ nonleptonic weak interactions [15]. This suppression of the $\Delta I = 3/2$ amplitude was explained by Miura-Minanikawa [16] and Pati-Woo [17] in terms of the colour symmetry of the valence quarks in the baryon. Thus, one is tempted to assume a dominance of $\Delta I = 1/2$ transitions also in the nonmesonic decay of the Λ-hyperon. It was observed, however, that theoretical calculations involving this assumption —*i.e.* only $\Delta I = 1/2$ transitions—

[a] e-mail: h.stroeher@fz-juelich.de

Table 1. The lifetimes of heavy hypernuclei from e^- and $\bar{p}$-induced reactions from refs. [18,19,11]. The numbers given in parenthesis represent the systematic errors.

Target & projectile	τ_Λ / ps	Ref.	Comment
Bi + e	2700 ± 500	[18]	
Bi + $\overline{p}$	250^{+250}_{-100}	[19]	
Bi + $\overline{p}$	180 ± 40 ($\pm$ 60)	[11]	Reanalysis of data from [19]
U + $\overline{p}$	130 ± 30 ($\pm$30)	[11]	

systematically underpredict the ratio Γ_n/Γ_p of nonmesonic decay rates induced by neutrons ($n+\Lambda \to n+n$) to the decay rates induced by protons ($p+\Lambda \to p+n$) [20]. Several attempts have been made to reconcile this discrepancy, *e.g.*, in refs. [21–26], but none of them has solved this problem in a convincing way.

This might lead to the conclusion that the contribution of the $\Delta I = 3/2$ transition to the nonmesonic decay of the Λ-hyperon is not negligible, *i.e.* the $\Delta I = 1/2$ rule could be violated [27–31]. The arguments presented in favor of this hypothesis in refs. [27–29,31] have been based essentially on the observed nonmesonic decay widths of the lightest hypernuclei. However, the experimental uncertainties are too large to allow for any definite conclusion. It is thus necessary to obtain information on the possible violation of the $\Delta I = 1/2$ rule from other properties of hypernuclei, *e.g.* from the mass dependence of the lifetime of hypernuclei as addressed in ref. [30].

As far as experiments are concerned, it can be stated from the inspection of table 1, that the data —with exception of the experiment performed with an e^- beam in Kharkov [18]— agree within the limits of errors. In ref. [32] it has been shown that a hypernucleus fraction decaying on a timescale of 2700 ps (as quoted in [18]) must be smaller by orders of magnitude compared to the fraction of hypernuclei decaying on timescales of 200 ps. However, the errors for τ_Λ in the measurements from [19,11] are so large that no severe constraints could be imposed on the various theoretical models for the nonmesonic decay.

In order to improve the situation, experiments with Au, Bi and U targets have been performed during the last years by the COSY-13 Collaboration at the Forschungszentrum Jülich using the internal proton beam of the COSY accelerator. We briefly describe the different stages of the proton-nucleus reactions —leading to hypernucleus formation and their delayed fission due to the $\Lambda N \to NN$ decay— in sect. 2. The experimental setup used to distinguish prompt and delayed fission events is sketched in sect. 3 and an overview of the experimental results for the Λ lifetime is given in sect. 4. In sect. 5 we discuss the implication of the latter results for the selection rule $\Delta I = 1/2$ in the $\Lambda N \to NN$ transition. A discussion of open problems and a summary are presented in sects. 6 and 7, respectively.

2 Heavy-hypernuclei formation in p + A reactions and their decays

In case of heavy hypernuclei the application of direct timing methods —as adopted for light hypernuclei— is not feasible due to the large background of light particles produced. This problem is circumvented by detecting heavy fragments from fission induced by the Λ-hyperon decay in heavy hypernuclei. The technique used is the recoil shadow method originally suggested by Metag *et al.* for the measurement of fission isomers [33]. It has also been employed by Armstrong *et al.* [11] in the lifetime measurements with antiprotons.

A novel approach to produce heavy hypernuclei for lifetime measurements —as performed by the COSY-13 Collaboration— is to use proton collisions on heavy targets like U, Bi or Au. The possibility to vary the beam energy allows to measure the background (at a low beam energy, *e.g.* of 1 GeV) concurrently with the effect (*e.g.*, at 1.9 GeV) by operating COSY in a supercycle mode, which has not been possible in the $\bar{p}$-induced reactions in [11]. Furthermore, a variation of the projectile energy in proton-induced reactions permits to find out whether production and decay of a fission isomer might fake the decay of a hypernucleus. Such a test is also not possible in antiproton-nucleus interactions since the center-of-mass energy is fixed for stopped antiprotons and always above threshold for Λ production. Furthermore, in $p + A$ reactions a large part of the proton momentum is transferred to the hypernucleus such that the surviving hypernuclei recoil faster than in $\bar{p}$-induced reactions; this increases the sensitivity of the recoil shadow method for lifetime measurements accordingly.

For illustration we show in fig. 1 the various stages and timescales involved in the $p + A$ reaction from i) the initial configuration to ii) the associated hyperon production in the target nucleus by pN inelastic scattering ($\sim 10^{-23}$ s), iii) Λ-hyperon capture in the residual nucleus via elastic ΛN scattering ($\sim 10^{-22}$ s), iv) the $\Lambda N \to NN$ reaction on the timescale of 200 ps leading to v) delayed fission of the hypernucleus. The right part shows the nucleon potentials during the various phases of the reaction.

Due to the complexity of these reactions the various stages illustrated in fig. 1 have been simulated by coupled-channel Boltzmann-Uehling-Uhlenbeck (CBUU) transport calculations for the fast nonequilibrium phase [34–37] followed by Hauser-Feshbach calculations for the statistical evaporation phase [38]. The transport model employed has been used for a variety of hadron-nucleus and nucleus-nucleus reactions from low to relativistic bombarding energies and been tested with respect to the overall reaction dynamics as well as the production of strange and nonstrange hadrons (for reviews see refs. [39,40]). The CBUU calculations provide information on i) the formation cross-section of "hot" hypernuclei as well as on ii) the properties of the hypernuclei produced —*i.e.* primary mass, charge, excitation energy, linear momentum, angular momentum etc.— in a given reaction. The latter information from the CBUU calculation then is used to evaluate (within Hauser-Feshbach calculations) for each event the subsequent

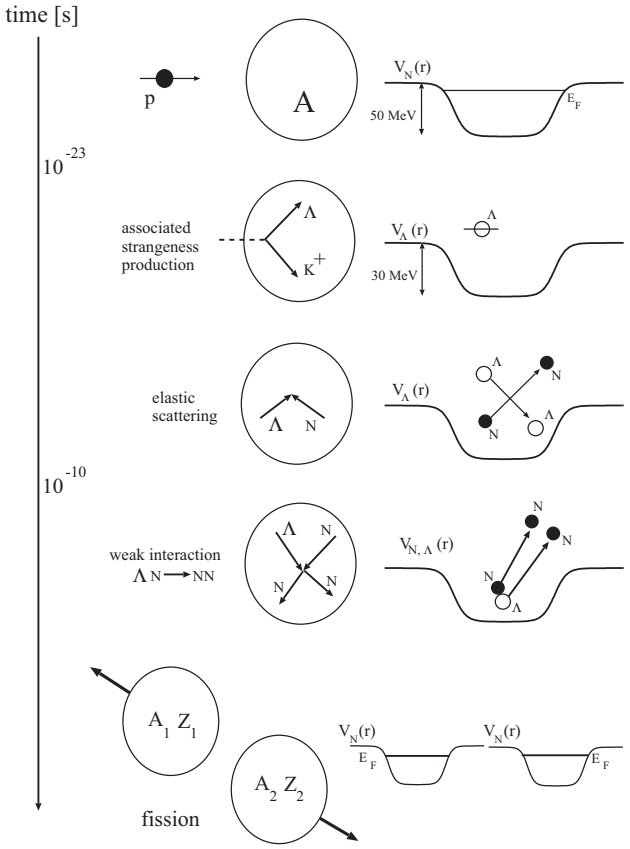

Fig. 1. Time evolution of a proton-nucleus collision from i) the initial configuration up to v) the delayed fission of a hypernucleus; ii) associated strangeness production; iii) elastic ΛN scattering; iv) decay of a Λ-hyperon via the $\Lambda N \to NN$ process leading v) to fission of the excited nucleus. The right part shows the nucleon potentials during the various phases.

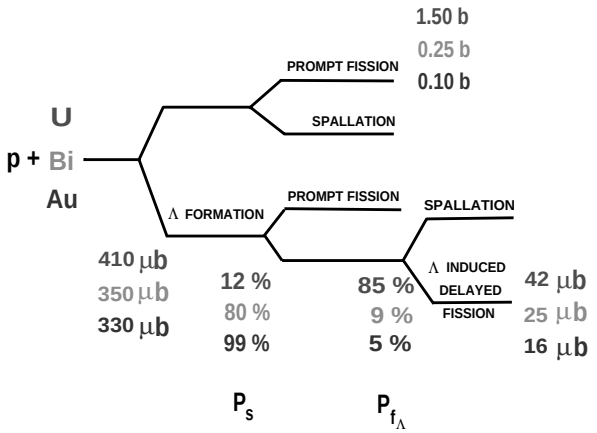

Fig. 2. Schematic representation of contributions from different competing processes in $p+$Au, $p+$Bi, $p+$U reactions at $T_p = 1.9$ GeV according to the CBUU + Hauser-Feshbach calculations (see text). The experimental cross-sections for prompt fission have been taken from refs. [43,44].

statistical decay as well as the probability P_s of a heavy hypernucleus to survive the competition with prompt fission [37]. Thus, the final distribution in mass and charge of the "cold" hypernuclei —reached after $\sim 10^{-18}$ s (see below)— is evaluated together with their individual (A, Z dependent) velocity distribution in the laboratory frame. The probability for delayed fission P_{f_Λ} —as induced by the $\Lambda N \to NN$ reaction for a hyperon from the S-state in the individual hypernuclei on a timescale of 200 ps— is calculated again within the Hauser-Feshbach formalism [37]. The kinematics of the fission fragments, furthermore, is simulated according to the Viola systematics [41] assuming isotropic angular distributions for the fission fragments in the rest frame of the decaying hypernucleus. For further details we refer the reader to refs. [36,37,42].

The cross-sections for Au, Bi, and U targets at $T_{\rm lab} = 1.9$ GeV —as calculated from the CBUU + evaporation calculations— are displayed in fig. 2, where we show the predicted cross-sections and branching ratios for all targets. The experimental cross-sections quoted in fig. 2 for prompt fission have been taken from refs. [43,44]. In contrast to the large differences in the prompt fission cross-sections, which amount to a factor of ~ 15 for U and Au targets, the cross-sections for delayed fission (~ 42, 25 and 16 μb for U, Bi and Au, respectively) are rather similar. This is due to the fact that the probability to observe the delayed fission of hypernuclei is determined by a product of two probabilities: the survival probability P_s of ("hot") hypernuclei against prompt fission and the probability P_{f_Λ} for fission of ("cold") hypernuclei induced by a Λ-hyperon decay. We find, that their product remains constant within a factor of 2-3.

The comparison of the cross-sections for delayed fission of hypernuclei and prompt fission of target nuclei in fig. 2 shows that in experiments with Bi and Au targets the same statistics for delayed fission fragments can be obtained using 2-3 times the beam time for a corresponding uranium experiment. On the other hand, the background from prompt fission in the Bi or Au experiments is much smaller because the ratio of the prompt to the delayed fission cross-sections is small compared to a U target. This reduces the load on the detectors in the prompt fission region for Au and Bi targets by about an order of magnitude relative to U. These expectations (calculations) were confirmed in the actual experiments at COSY-Jülich using Bi [32], Au [45] and U targets [46], where similar cross-sections were observed experimentally.

Another important ingredient for the data analysis (to be discussed later) is the velocity distribution of the hypernuclei in the laboratory. The latter is dominantly determined by the nucleon-nucleon and hyperon-nucleon cross-section in the initial stage of the reaction as modeled by the CBUU approach. It has been shown in comparison to independent experimental data from refs. [47,48] that the momentum transfer to the residual nucleus is well described by the transport approach in $p+$U reactions for $T_{\rm lab} = 0.5$–3 GeV [46].

During the statistical decay phase the hypernucleus velocity distributions change only moderately, however, a very pronounced change in the mass and charge distributions is observed [37]. The final charges and masses

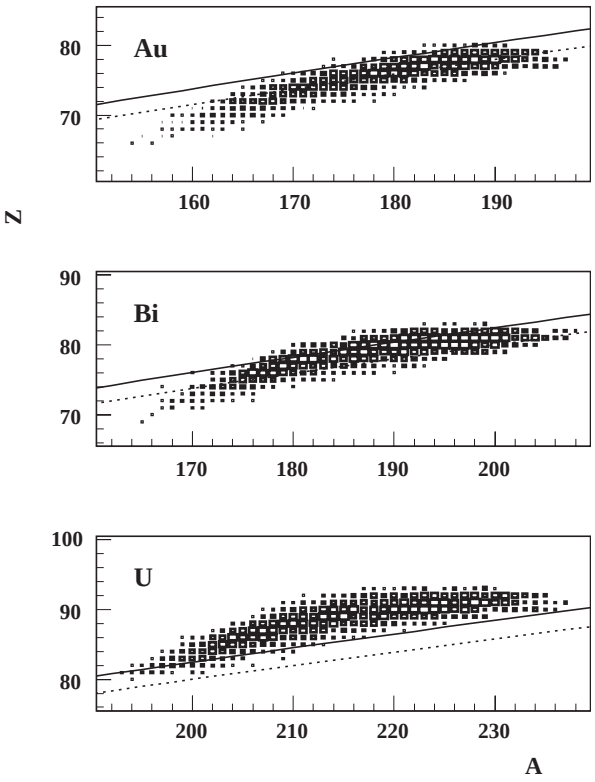

Fig. 3. Two-dimensional spectra from CBUU + evaporation calculations in charge Z and mass A of hypernuclei for $p+$ ^{197}Au at $T_p = 1.7$ GeV, $p+$ ^{209}Bi at $T_p = 1.9$ GeV and $p+$ ^{238}U at $T_p = 1.9$ GeV. The solid and dotted lines indicate hypernuclei of fissility $Z^2/A = 34$ and 32, respectively. Delayed fission events essentially stem from nuclei with fissility parameter $Z^2/A \geq 34$.

of "cold" hypernuclei are correlated to form a "valley of stability". The resulting two-dimensional spectra in charge Z and mass A of cold hypernuclei (typically, after 10^{-18} s) are shown in fig. 3 in terms of cluster plots. These differential distributions represent CBUU + evaporation model calculations for hypernuclei produced in the reactions $p+$ ^{197}Au at $T_p = 1.7$ GeV, $p+$ ^{209}Bi at $T_p = 1.9$ GeV, $p+$ ^{238}U at $T_p = 1.9$ GeV. It is seen that the two-dimensional plots are quite similar for the three reactions considered, but shifted in mass and charge according to the initial target. It should be noted that the width of the distribution in charge Z remains rather constant as a function of mass A. This can be inferred directly from the isospin-independent emission of protons and neutrons in the pre-equilibrium CBUU collision stage before the Coulomb barrier is formed; after that the proton emission is suppressed by the Coulomb barrier and neutron emission fills out the "valley of stability".

Figure 3 shows that although the distributions in mass differ by about 10 to 30 units for the different targets, they have some common overlap region in the tails. Furthermore, the Λ-induced fission probability essentially depends on the fissility parameter Z^2/A (see fig. 3). The solid and dotted lines in fig. 3 show hypernuclei of $Z^2/A = 34$ and 32, respectively. We recall that only a fraction of the (A, Z) distributions of hypernuclei created in $p + A$ interactions actually lead to delayed fission events (see $P_{f\,\Lambda}$ in fig. 2), *i.e.* essentially for $Z^2/A \geq 34$. When averaging over the experimental results for all targets one thus obtains a value for τ_Λ that corresponds to an average over all nuclei with masses $A \geq 180$.

3 Experimental setup and data analysis

Hypernuclei produced in proton-nucleus collisions, which survive the prompt fission stage, leave the target with a recoil velocity v_R. They subsequently decay at some distance from the target proportional to the lifetime τ_Λ of the Λ-hyperon and to the velocity v_R. Thus, prompt and delayed fission events can be separated by the spatial distribution of their decays. The problem, however, is that the prompt fission events are more frequent than the delayed fission processes by factors of up to 10^5 (cf. fig. 2) —which corresponds to the ratio of prompt to delayed fission cross-sections— and the spatial distribution of delayed events has to be measured with high accuracy. The particular solution to this problem is provided by the recoil shadow method [33], which allows to analyse the spatial distribution of delayed decays with respect to the product $\tau_\Lambda \cdot v_R$ in the presence of a huge background compared to the investigated effect.

A schematic view of the detection scheme [49] is shown in fig. 4, where the dimensions of the target and its holder —serving as a diaphragm— are increased by a factor ≈ 30 in comparison to the dimensions of the low-pressure multiwire proportional chambers (MWPC) placed 30 cm from the target in a direction perpendicular to the target. The multiwire chambers are sensitive to fission fragments, but not to protons and other light particles. These detectors were partly screened by the target holder such that the prompt fission fragments —originating from the target— could not hit the (left) shadow part of the detector. This was, however, possible for fragments from the delayed fission of hypernuclei $_\Lambda A$ escaping from the target downstream the beam and fissioning in some distance from the target. A schematic event distribution —projected onto the beam axis— is shown in the upper part of fig. 4. It is characterized by an exponential fall-off for the delayed fission events in the shadow region and a constant (prompt) yield in the bright (right) region of the detector. For further details we refer the reader to ref. [49].

In order to check whether the events detected in the shadow region are not light particles or even γ's, the following test measurements have been performed:

- The MWPC were irradiated with minimum ionizing particles (γ's and e^-); it was shown that the detection efficiency for such particles is below 10^{-11}.
- A pure carbon foil was used as a target in $p + A$ reactions, leaving the detection system unchanged. The measured spectra in the shadowed part of the detectors were found to contain no events.

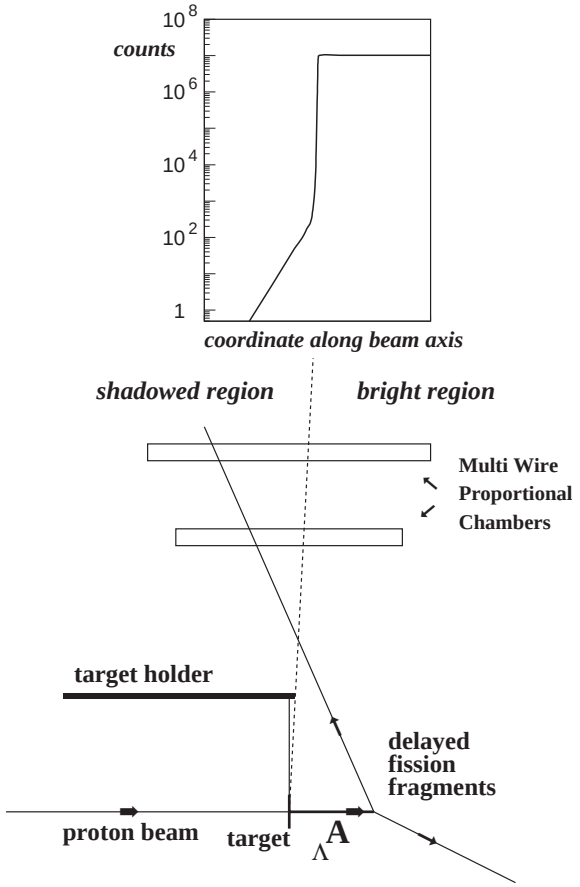

Fig. 4. Schematic view of the experimental setup and illustration of the recoil distance method (see text). The dimension of the target holder and target in the lower part are increased by a factor ≈ 30 relative to the MWPCs.

– A ^{252}Cf source was placed at the target position and a two-dimensional energy loss *versus* time-of-flight spectrum between both MWPC was measured. The results were found to be in agreement with Monte Carlo simulations, taking into account the mass, charge and velocity distributions of fragments according to the Viola systematics [41] for spontaneous fission of californium.

The fragments that hit the shadow part (left) of the detector thus originate either from the delayed fission of hypernuclei (or hyperfragments) or they are emitted in prompt fission from the target, which, due to scattering on the shadow edge of the target holder, have changed their initial trajectories. Therefore, scattering in fact creates a background in the shadow region with an intensity proportional to the prompt fission cross-section. In order to determine the background distribution of hits in the shadowed part of the detector, measurements have been performed at a much lower proton energy ($T_p = 1.0$ GeV), where the cross-section for hypernucleus production is expected to be negligibly small (about 4 orders of magnitude smaller than at 1.9 GeV), whereas the prompt fission yield is about the same. The scattering of fragments from prompt fission on the target holder which creates background for the delayed fission fragment distribution could, in principle, depend on the energy if the momentum transfer would change significantly with beam energy. As evident from experimental data of Kotov *et al.* [48] for proton-induced fission of U at 1.0, 1.5, and 2.9 GeV beam energy, this is, however, fortunately not the case for the energy range of our experiments.

It has been shown by Monte Carlo simulations that hyperfragments from prompt fission of hypernuclei, which have changed their direction due to the recoil induced by a subsequent Λ-hyperon decay, can hit the shadow region of the detectors only in a very narrow region (corresponding to about 1-2 mm close to the shadow edge in the MWPC) and thus do not contribute to the distribution that was actually used for the extraction of the lifetime of hypernuclei (see below).

The proton beam (with typically $5 \cdot 10^{10}$ protons in the COSY-ring) has been accelerated up to 1.9 GeV (for hypernucleus production) and to 1.0 GeV (for an estimation of the background originating from scattered fragments from prompt fission of the target nucleus). The COSY accelerator was operated in a supercycle mode, *i.e.* there were three cycles (each of ~ 15 s duration) of beam acceleration and irradiation of the target; two of them at the energy of 1.9 GeV and one at 1.0 GeV. This allowed to study the effect and the background concurrently for the same shape and thickness of the target.

In the analysis, the distribution of hit positions of the fission fragments on the surface of the detector were projected onto the beam direction. The respective distributions for the Au, Bi, and U target are shown in the upper parts of figs. 5, 6, 7 at $T_p = 1.9$ GeV (full dots) together with the background measured at $T_p = 1.0$ GeV (open circles).

These experimental distributions then have been compared with simulated distributions, which were evaluated assuming the velocity distribution of the hypernuclei (as obtained from the CBUU + Hauser-Feshbach calculations) and a lifetime of the Λ-hyperon in the hypernuclei, where the latter was treated as a free parameter in the fit procedure. For the details of the theoretical calculations with respect to the velocity distributions and a comparison with the available experimental data we refer the reader to ref. [46]. Since the number of events in the position distributions was not very large in some experiments, a Poisson instead of Gaussian probability distribution $p(n_i)$ has been used to obtain the number of counts n_i for each position bin (cf. ref. [46]). Then the best lifetime τ_Λ was deduced by the "maximum-likelihood" method, which allows also for an estimate of the statistical error for τ_Λ (see, *e.g.*, ref. [9]). The results of the fits are shown in the lower part of figs. 5, 6, 7 by the solid lines in the shadow region in comparison to the experimental data, where the background (measured at $T_p = 1.0$ GeV) has been subtracted from the 1.9 GeV data.

The question arises, whether the velocity distributions of hypernuclei might differ significantly when varying

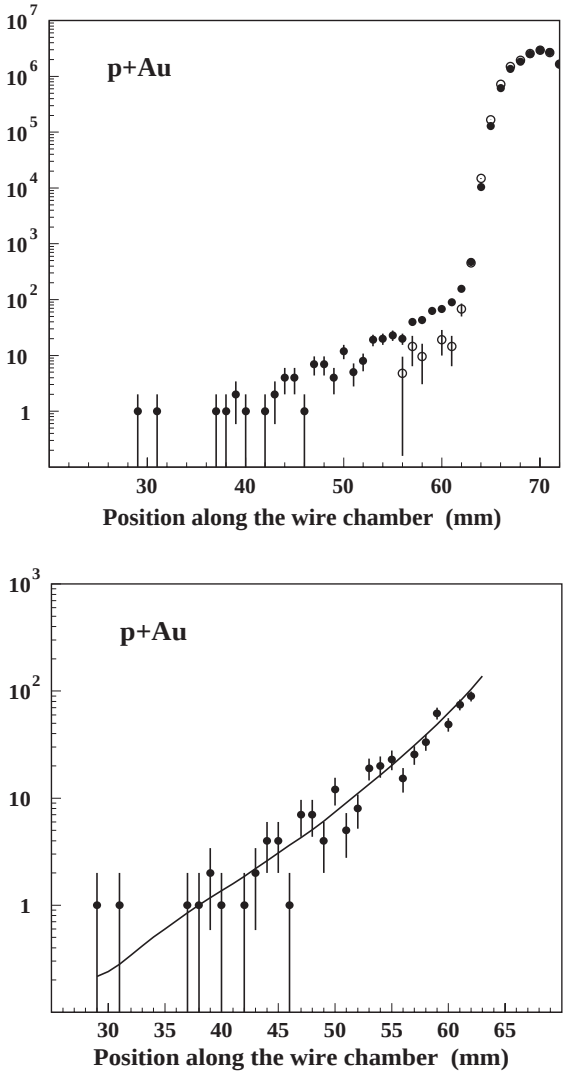

Fig. 5. Upper part: position distribution of hits of fission fragments in the position-sensitive detectors for the $p+\mathrm{Au}$ experiment (from ref. [45]). The full dots represent the data for $T_p = 1.9$ GeV, whereas the open circles show the data for $T_p = 1.0$ GeV normalized to the bright part of the detectors of the 1.9 GeV data. Lower part: position distribution of hits from delayed fission fragments of hypernuclei in the shadow region obtained by subtracting the background (normalized data taken at 1.0 GeV) from the data measured at 1.9 GeV. The solid line shows the result of the simulation with the extracted value for the lifetime according to the maximum-likelihood method.

(A, Z). In such a case the simulation of the position distributions, which is the crucial part in the analysis of the experimental data, would have to be carried out by folding the velocity distributions of hypernuclei with specified (A, Z) with the fission time distributions of these hypernuclei. However, as detailed calculations have shown [42], those hypernuclei which finally lead to fission, have very similar velocity distributions so that no corrections are necessary.

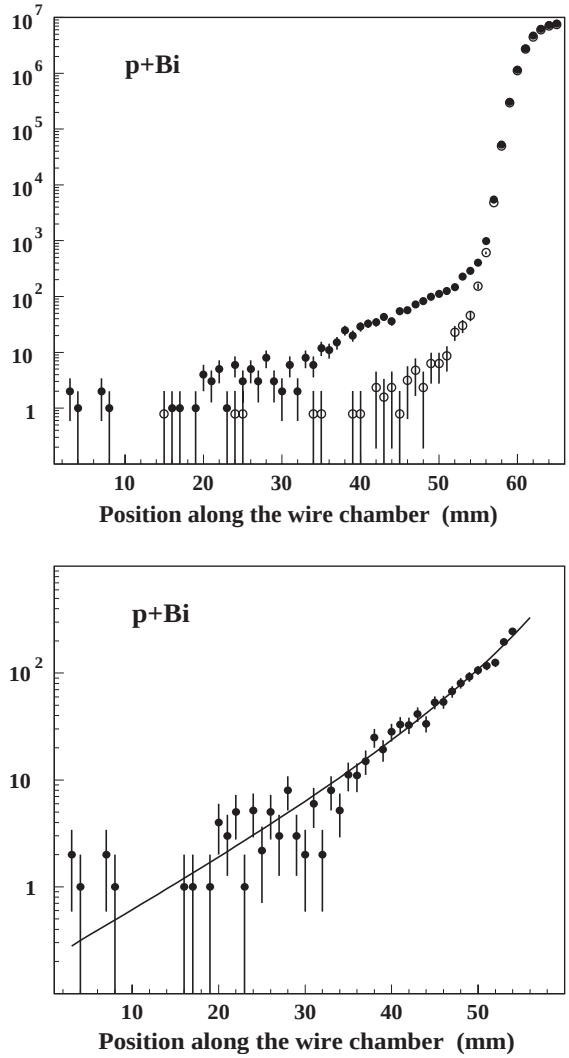

Fig. 6. The same distributions as in fig. 5 for the $p+\mathrm{Bi}$ experiment (from ref. [32]).

4 Summary of experimental results and error analysis

In this section we summarize the results of the COSY-13 Collaboration and compare to the lifetimes measured before (cf. table 1). Such a comparison must necessarily also involve a discussion of experimental uncertainties. Whereas the *statistical* errors can be unambiguously determined by the maximum-likelihood method as described in detail in ref. [46], the estimation of *systematic* errors has to be discussed individually for each experiment, since the number of events in the shadow region of the detectors have been different as well as the stability of the individual targets during the irradiation periods.

4.1 Systematic errors

The systematic errors arise from:

a) the velocity distribution of hypernuclei,

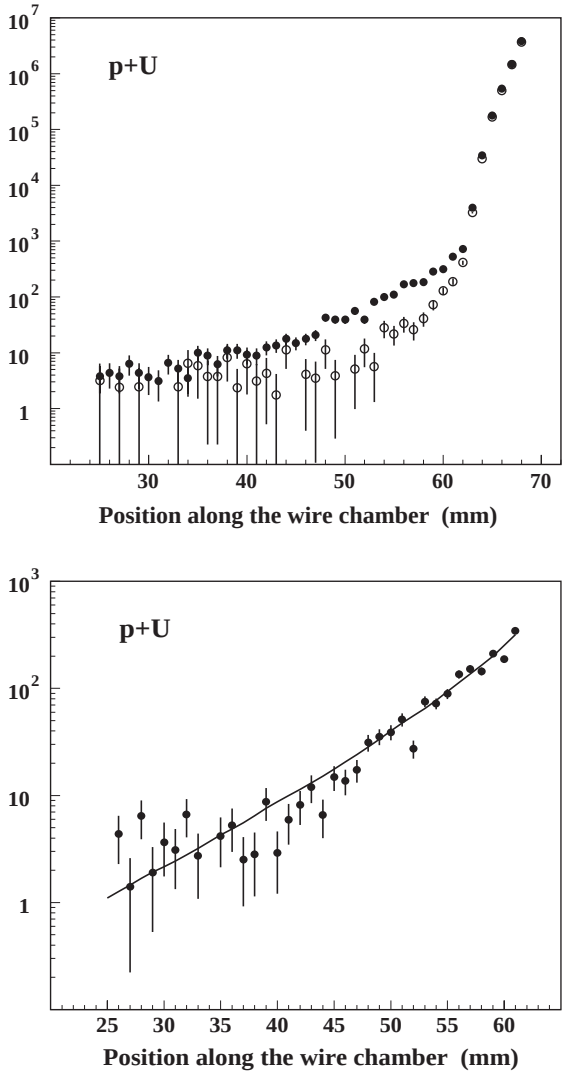

Fig. 7. The same distributions as in fig. 5 for the $p+\mathrm{U}$ experiment (taken from ref. [46]).

b) the nonisotropic emission of the fission fragments,
c) the nonuniform irradiation of the target by the proton beam,
d) the change of position and shape of the targets during the measurements,
e) the background treatment in case of low statistics, and
f) the explicit search procedure (χ^2 or maximum-likehood methods) for the best lifetime.

Detailed simulations have been carried out to determine the possible variations in the lifetime τ_Λ according to the error sources listed above. The results of these studies in ref. [46] lead to the actual numbers shown in table 2 for the three individual targets.

The total systematic error can be summed up to 15 ps for the Au target, to 14 ps for the Bi target, and to 17 ps for the U target.

Table 2. The sources of systematic errors in the COSY-13 experiments. The total systematic error has been evaluated assuming that the sign of all contributions is the same.

Source of errors	Au	Bi	U
a) velocity distribution	2 ps	2 ps	2 ps
b) anisotropic emission	2 ps	2 ps	2 ps
c) nonuniform irradiation	4 ps	4 ps	4 ps
d) change of shape and position	2 ps	1 ps	4 ps
e) background treatment	3 ps	3 ps	3 ps
f) search procedure	2 ps	2 ps	2 ps
Total	15 ps	14 ps	17 ps

Table 3. The lifetime of heavy hypernuclei measured at COSY-Jülich by COSY-13. The errors in the third column have been obtained by quadratically adding the statistical and systematic errors from the second column.

Target	τ_Λ (ps)	τ_Λ (ps)	Ref.
Au	130 ± 13(stat.)$\pm$15(syst.)	130 ± 20	[45]
Bi	161 ± 7(stat.)$\pm$14(syst.)	161 ± 16	[32]
U	138 ± 6(stat.)$\pm$17(syst.)	138 ± 18	[46]

4.2 Results

We recall that due to the rather large dispersion in the (A, Z) distribution of cold hypernuclei (cf. fig. 3) the observation of the delayed fission of these nuclei does not allow to deduce the lifetime of specific heavy hypernuclei, *i.e.* with fixed atomic number Z and mass A, but it rather provides a lifetime averaged over a group of different hypernuclei.

A summary for the lifetimes τ_Λ including the statistical and systematic errors is presented in table 3. It can be concluded that the experiments performed with the proton beam on Au, Bi, and U targets give consistent and comparable values for the lifetime of heavy hypernuclei. Within errors these values are identical, though the average masses of the fissioning hypernuclei differ for the different targets (cf. fig. 3). On the other hand, the individual distributions in (A, Z) overlap such that we may also average over the three experiments to obtain an average lifetime for hypernuclei with masses $A \approx 180$–225 with a dispersion in charge $\Delta Z \approx 3$ (for fixed A) as

$$\tau_\Lambda = 145 \pm 11 \text{ ps} \qquad (\text{for } p + A)\,.$$

The average lifetime and its error were obtained by weighting the experimental lifetimes for the individual targets with the reciprocals of the statistical and systematic errors added quadratically, *i.e.* by the reciprocals of the squares of the errors listed in the third column of table 3. Due to a nonuniform irradiation of the targets the changes in the shape and position of the targets —during the measurements— as well as the background conditions were different and thus not correlated for the

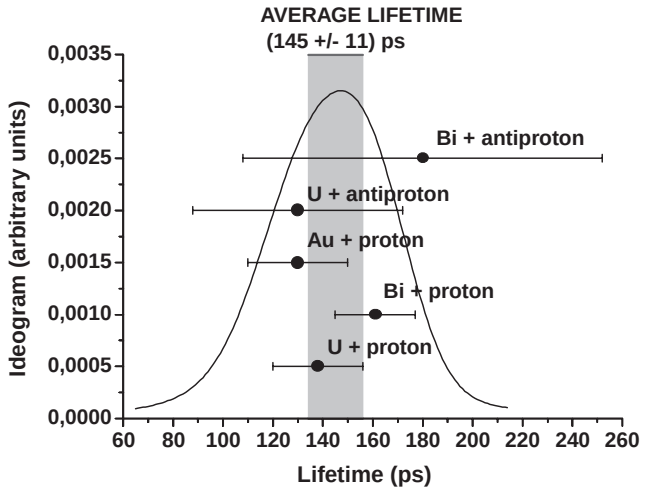

Fig. 8. The lifetimes for proton- and antiproton-produced hypernuclei on Au, Bi and U targets. The horizontal bars present the statistical and systematic errors added in quadrature. The gray vertical bar displays the overall average value for the lifetime of heavy hypernuclei and its width shows the error. The smooth Gaussian-like curve was evaluated as proposed in the Review of Particle Physics [9], *i.e.* adding Gaussian curves representing results from individual experiments. Parameters of these Gaussian curves (average value and standard deviation) are equal to the individual lifetimes and their errors (square roots from sum of squares of statistical and systematic errors). The weights —with which the individual curves enter the sum— were chosen as reciprocals of the errors quoted above. The smoothness of the resulting curve indicates the internal consistency of the different data.

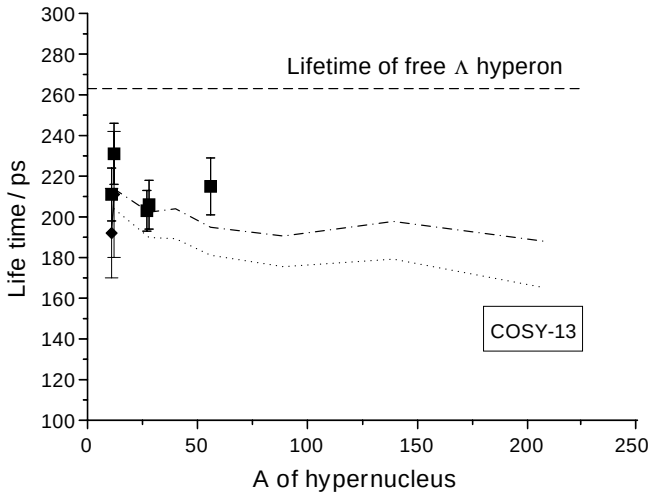

Fig. 9. Mass dependence of the Λ lifetime. Diamonds and squares represent experimental data obtained for light hypernuclei in refs. [5,6] and [8,50], respectively. The rectangle at $A \sim 200$ represents the summarized experimental result obtained for heavy hypernuclei by the COSY-13 Collaboration. The width of the rectangle indicates the range of masses of the hypernuclei observed in the different COSY-13 experiments ($180 \leq A \leq 225$), whereas the height corresponds to the experimental accuracy quoted in the text (11 ps). The dot-dashed line and dotted line present results of theoretical calculations from refs. [51] and [52], respectively, while the horizontal dashed line shows the experimental lifetime of the free Λ-hyperon.

different experiments. We, therefore, have assumed that the systematic errors for these three measurements are not correlated.

4.3 Comparison with antiproton-induced reactions

This average lifetime of heavy hypernuclei is within the statistical error limits in agreement with the lifetimes extracted from antiproton experiments refs. [11] (see table 1), which by averaging over the Bi and U targets amounts to

$$\tau_\Lambda = 143 \pm 36 \text{ ps} \qquad (\text{for } \overline{p} + A).$$

In fact, the mass and charge distribution of hypernuclei from the experiments with antiprotons should be similar to those of the proton-induced reactions, since a comparable amount of energy is transferred to the nucleus. However, the latter reactions lead to a much more precise value for τ_Λ since i) the background can be determined experimentally in contrast to the $\bar{p}$-induced reactions — which reduces the systematic errors— and ii) the velocity of the hypernuclei is much larger in the laboratory due to the higher momentum transfer from the proton at $T_p = 1.9$ GeV. This fact also leads to a cleaner separation of delayed fission events from prompt fission events in the shadow region of the detector that stem from small-angle scattering on the target holder. Moreover, the geometrical conditions of proton-induced reactions allow for a less ambiguous interpretation of fission fragment distributions in the shadow regions of the detectors than those for antiproton experiments because in the former investigations it was possible to neglect the contribution of hyperfragments which originate from prompt (not delayed) fission of hypernuclei, but are observed in the shadow region due to recoil caused by subsequent decay of the Λ-hyperon.

A compilation of all results discussed above for the lifetime τ_Λ from proton- and antiproton-induced reactions is presented in fig. 8 in the form proposed in the Review of Particle Physics [9]. We note that adding the result from the $\bar{p}$ experiments to the data from COSY-13 does not change the number of $\tau_\Lambda = 145 \pm 11$ ps quoted above.

5 Implications for the ΛN → NN reaction

The mass dependence of hypernucleus lifetimes is shown in fig. 9. The experimental results for light hypernuclei (mass number $11 \leq A \leq 56$) seem to be independent of the mass number within the limits of errors. The lifetimes of heavy hypernuclei as measured by the COSY-13 Collaboration do not indicate a mass dependence in the studied range of mass numbers ($180 \leq A \leq 225$) either. However, experimental results show that the lifetimes of heavy hypernuclei are shorter by $\sim$ 60–70 ps than those

for light hypernuclei. This difference implies that the lifetime should decrease by less than 0.5 ps per mass unit. Such a weak decrease could not be established within the present experimental accuracy if the light or the heavy hypernuclei are studied separately. In both cases, the covered mass range is about 45 mass units corresponding to a variation of the lifetime by about 20 ps, *i.e.* less than two experimental errors.

The dotted and dot-dashed lines in fig. 9 represent theoretical model expectations evaluated within the meson exchange model. In both calculations the validity of the $\Delta I = 1/2$ rule has been assumed and the contribution from nonmesonic decays initiated by two nucleons was included. Nevertheless, the results of the calculations differ rather significantly, *i.e.* ~ 10 ps for light and ~ 20 ps for heavy hypernuclei.

Most important, however, a smooth decrease of the lifetime *versus* mass of the hypernuclei is a common property of both model calculations, *i.e.* both approaches reproduce qualitatively the mass dependence of the experimental data as extracted from the comparison of lifetimes of light and heavy hypernuclei. Furthermore, both models predict a weaker decrease of the lifetime with mass than observed in the experiment. The calculations of Alberico *et al.* [51] lead to a difference between the largest lifetime (for ${}^{12}_{\Lambda}$C) and the smallest one (for ${}^{208}_{\Lambda}$Pb) of about 26 ps. Similarly, this difference in the model of Jido *et al.* [52] is 39 ps, whereas the difference in the average experimental lifetimes from light and heavy hypernuclei is approximately 60–70 ps. Such a large discrepancy between theory and experiment indicates that at least one of the model assumptions is inadequate.

As discussed in the introduction and demonstrated in ref. [30], the $\Delta I = 1/2$ rule could be violated in the $\Lambda N \to NN$ interaction contrary to the case of free hyperon decays. In this respect, we recall that the lifetime of heavy hypernuclei is sensitive to the ratio R_n/R_p of the neutron-induced to proton-induced Λ nonmesonic decays $\Lambda + N \to N + N$, whereas the lifetime of light hypernuclei ($A \approx 12$) is independent of this ratio. Thus, a precise knowledge of the lifetime of light hypernuclei (which depends only on $R_n + R_p$) and an accurate knowledge of the lifetime of heavy hypernuclei (depending both on $R_n + R_p$ and on R_n/R_p) enables us to determine the absolute normalization, *i.e.* $R_n + R_p$, as well as the ratio R_n/R_p.

Furthermore, we can test the validity of the phenomenological $\Delta I = 1/2$ rule due to the following reasons: The ratio R_n/R_p vanishes for final state isospin $I_f = 0$ since the neutron-induced Λ decay leads only to neutron-neutron final states, which cannot form an isospin zero state. On the other hand, the ratio R_n/R_p is equal 2 for $\Delta I = 1/2$ decays to pure $I_f = 1$ final states (realized, *e.g.*, for Λ-nucleon spin state S) [29]. Therefore, in the general situation —where the observed decays correspond to an incoherent mixture of the $I_f = 0$ and $I_f = 1$ final states— pure $\Delta I = 1/2$ decays must always result in a ratio $R_n/R_p \leq 2$. Any measured ratio $R_n/R_p \geq 2$ then will indicate a violation of this rule. We will argue in the following that this should be indeed the case.

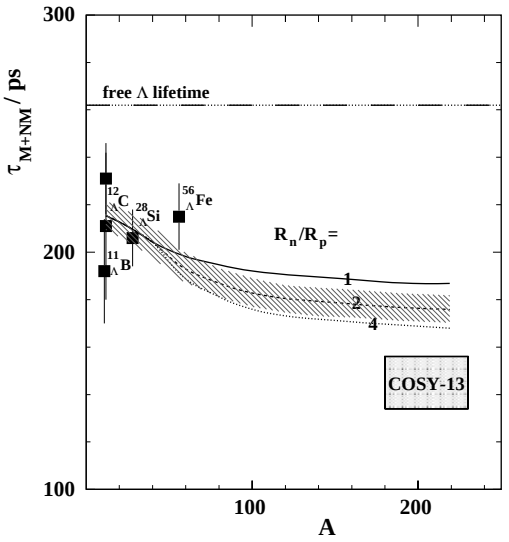

Fig. 10. Calculations of the Λ lifetime $\tau_{\rm M+NM}$ due to the mesonic and nonmesonic decay as a function of the cold hypernucleus mass A (from ref. [30]) in comparison to the data of refs. [8,6]. The COSY-13 Collaboration result for nuclei with masses $A \geq 180$ is marked by the hatched area labelled "COSY-13". The width and height of this rectangle represent the mass range of hypernuclei involved and the error of the lifetime determination, respectively. In the theoretical calculations both mesonic and nonmesonic decay modes are taken into account, whereas the unknown ratio of the weak decay rates R_n/R_p is treated as a parameter with values $R_n/R_p = 1$, 2, and 4. The hatched area around the dashed line (corresponding to $R_n/R_p = 2$) shows the $\pm\sigma$ uncertainty in the magnitude of the weak transition $\sim (R_n + R_p)$ determined from the lifetimes of light hypernuclei with $A \approx 12$.

To strengthen these arguments, we show again in fig. 10 the theoretical calculations from ref. [30] for the Λ-hyperon lifetime as a function of the hypernucleus mass A, where both the mesonic and nonmesonic contributions are included. In these calculations the strength of the weak transition $\Lambda N \to NN \sim R_n + R_p$ is fixed in magnitude to the data (cf. fig. 10) for light hypernuclei with $N \approx Z$ and masses $A \approx 12$. We mention that this strength has an error of about 5% according to a statistical analysis of the lifetimes for these nuclei which amounts to $\approx \pm 7$ ps for heavy hypernuclei ($A \sim 200$).

The calculations for a constant ratio R_n/R_p then lead to a smooth decrease for the lifetime as a function of mass A which approximately saturates for $A \approx 160$ (solid line for $R_n/R_p = 1$). When increasing the ratio to $R_n/R_p = 2$ we obtain the dashed line which is the lower limit for the $\Delta I = 1/2$ rule to hold according to the arguments presented above. Any further increase of R_n/R_p (dotted line) leads to a steeper dependence of τ_Λ with mass A since in neutron-rich nuclei —along the line of stability— the $n\Lambda \to nn$ channel becomes the dominant one.

When comparing the different theoretical lines with the lifetime extracted from the present work for masses $A \geq 180$ (hatched area with COSY-13), we find that a ratio $R_n/R_p \leq 2$ is not compatible with $\tau_\Lambda = 145 \pm 11$ ps

for the heavy hypernuclei. Thus, within the scenario described above, the $\Delta I = 1/2$ rule is violated.

The latter conclusion also holds, when the contribution of two-nucleon induced decays ($\Lambda + n + p \rightarrow n + n + p$) is taken into account, since it was shown by Ramos *et al.* [23] that the yield of two-nucleon induced decays of Λ-hyperons is independent of the mass of the hypernucleus. The presence of such a mass-independent contribution effects the mass dependence of lifetimes in the same way as a decrease of the R_n/R_p ratio, *i.e.* it makes the mass dependence less steep. Therefore, an experimental indication for a steeper mass dependence relative to the theoretical result for the one-nucleon induced decay — under the assumption of the validity of the $\Delta I = 1/2$ rule— becomes an even stronger argument for a violation of this rule when two-nucleon induced decays contribute.

Since this conclusion is based on experimental data for lifetimes of light and heavy hypernuclei, which are biased by statistical and systematic errors, the possible violation of the $\Delta I = 1/2$ rule can only be stated with some confidence level $P_c < 1$. To estimate this probability we followed the error analysis described in ref. [30] using the present average value for the lifetime of heavy hypernuclei (cf. fig. 10) with the error evaluated as a sum of statistical and systematic errors (11 ps). This leads to a confidence level ≈ 0.98; an inclusion of the antiproton data from ref. [11] (table 1) does not modify this result.

It should be emphasized that the mass dependence of the lifetime varies only weakly with the ratio R_n/R_p for large values of this ratio. Thus the error in the normalization of the theoretical curves in fig. 10, *i.e.* ± 7 ps —the error of $R_n + R_p$ determined by the accuracy of the lifetimes of light hypernuclei— and the error of the lifetime for heavy hypernuclei, *i.e.* ± 11 ps (as extracted from the COSY-13 data) do not allow to establish the ratio R_n/R_p more precisely; it can only be stated that it is larger than 2.

6 Discussion

The conclusions presented above rely on: i) the accuracy of the overall normalization, which is a free parameter of the present theoretical model, and ii) the assumption that the model predictions with respect to the mass dependence of the hypernuclei lifetimes are reliable. We will discuss these premises in the following.

We recall that the theoretical model formulated in ref. [30] is based on the transport Boltzmann-Uehling-Uhlenbeck equation (BUU). It treats the nuclei as systems of fermions in a self-consistent mean field with mutual in-medium interactions allowed by the Pauli principle. Due to the semiclassical limits invoked, the approach neglects the shell structure of the nuclei.

The decay width of the nonmesonic decay is evaluated from the collision rate of hyperons with nucleons in the target using local Thomas-Fermi distributions for the nucleon phase space density and a 1s state wave function for the hyperon. Since the cross-section for the $\Lambda + N \rightarrow N + N$ weak process is not known from experiment, it was assumed in ref. [30] that the differential cross-section for the weak $\Lambda + N \rightarrow N + N$ process is proportional to the cross-section of elastic $\Lambda + N \rightarrow \Lambda + N$ scattering. This is the most far-reaching approximation of this model, which may influence both the normalization of the mass dependence of τ_Λ and the shape of this mass dependence.

i) The absolute normalization —a free parameter of the model— is responsible for all mass-independent factors. It has been determined from a comparison of the experimental and theoretical results for light hypernuclei, where our model results do not depend on the ratio R_n/R_p. In detail: The normalization has been performed to an average value of the lifetimes for ${}^{11}_{\Lambda}\mathrm{B}$ and ${}^{12}_{\Lambda}\mathrm{C}$ [9,8,6]. Within this normalization the confidence level for a violation of the $\Delta I = 1/2$ rule is found to be ~ 0.98. Taking the experimental lifetimes for ${}^{12}_{\Lambda}\mathrm{C}$ and for ${}^{11}_{\Lambda}\mathrm{B}$ [9,6] separately gives confidence levels of 0.99 and 0.95 for a normalization to ${}^{12}_{\Lambda}\mathrm{C}$ and to ${}^{11}_{\Lambda}\mathrm{B}$, respectively. This shows, that the uncertainty in the normalization cannot change the conclusion concerning the possibility of a violation of the $\Delta I = 1/2$ rule.

ii) However, as mentioned above, the lack of knowledge of the elementary cross-section for the weak $\Lambda + N \rightarrow N + N$ process might influence the shape of the mass dependence of τ_Λ.

To check the sensitivity of τ_Λ on the elementary cross-section for the weak $\Lambda + N \rightarrow N + N$ process, the calculations have been performed also with a constant (energy-independent) cross-section and compared with the results of ref. [30]. It was found that the mass dependence for the energy-independent cross-section turned out to be even flatter and the lifetimes for heavy hypernuclei increased by ~ 13 ps. Such a limit increases the difference between the experimental lifetime of heavy hypernuclei and the theoretical model and thus more strongly supports a violation of the $\Delta I = 1/2$ rule.

Furthermore, to explore the least favorable situation for rejecting the validity of the $\Delta I = 1/2$ rule, *i.e.* assuming a much steeper mass dependence, we have evaluated the confidence level for the case, where the limiting curve for $R_n/R_p = 2$ is shifted downwards by 20 ps for heavy hypernuclei. Even for such a significant modification of the model the confidence level is still quite large, ~ 0.75, in favor of a violation of the $\Delta I = 1/2$ rule.

To gain further insight into the validity of our theoretical model we have addionally compared the mass dependence of the hypernucleus lifetime from ref. [30] with the mass dependence from the more recent calculations of W.M. Alberico *et al.* [51] and D. Jido *et al.* [52]. Since in both studies the validity of the $\Delta I = 1/2$ rule has been assumed, we compare the mass dependence from ref. [30] within the same assumption (*i.e.* the limiting value $R_n/R_p = 2$ has been adopted) and omitted the contribution of two-nucleon induced Λ-hyperon decays in the results of refs. [51] and [52], since the model of ref. [30] does not include this contribution.

The calculated results for the mass dependence of τ_Λ from these three models are presented in fig. 11, where the squares correspond to the calculations of ref. [51], the

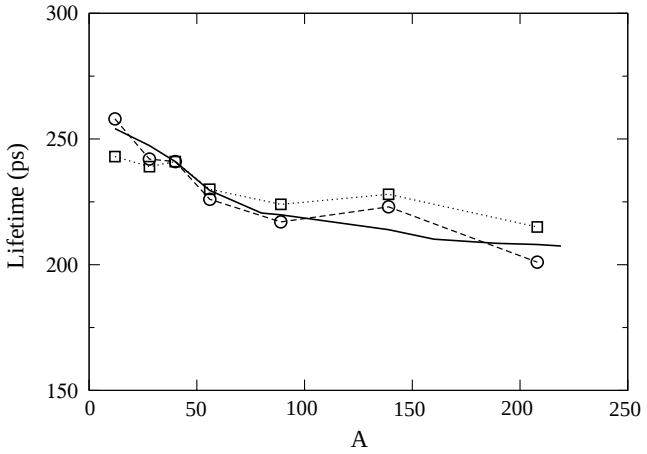

Fig. 11. Mass dependence of the Λ lifetime $\tau_{\mathrm{M+NM}} = 1/(\Gamma_{\mathrm{M}} + \Gamma_1)$ due to the mesonic and nonmesonic decay induced by single nucleons —as evaluated in refs. [51] (squares) and [52] (circles)— in comparison with the mass dependence calculated in ref. [30] for $R_n/R_p = 2$ and normalized with respect to each other at $A = 40$.

circles to the calculations of ref. [52] while the solid line shows the mass dependence from ref. [30] after normalization to the lifetime of ${}^{40}_{\Lambda}$Ca, which is predicted by the two other approaches to be exactly the same. The agreement of the mass dependence from ref. [30] with the results of the two other works is quite remarkable. In our opinion this points towards a satisfactory reliability of the phase space model [30].

We thus conclude that, in spite of the uncertainty in the shape as well as the uncertainty in the overall normalization of the theoretical mass dependence of $\tau_\Lambda(A)$, the experimental lifetime from COSY-13 is small enough to derive valid conclusions concerning a violation of the $\Delta I = 1/2$ rule.

Our conclusions —which specify that the ratio of neutron-induced to proton-induced weak decays of the Λ-hyperons in heavy hypernuclei is larger than 2— should be confronted with available results obtained from experiments, where the ratio Γ_n/Γ_p was measured by a straightforward detection of nucleons from the decay of hypernuclei. These results are shown in table 4.

The data for heavy hypernuclei on this ratio have been obtained in refs. [12–14] by using photographic emulsions to observe the decays of heavy hypernuclei in the mass range 40–100. An analysis of the energy spectra of fast protons was used for this purpose. In all these works a dominance of neutron-induced over proton-induced decays has been reported with a Γ_n/Γ_p ratio in the range from 1.5 to 9.0, which is in line with our findings.

On the other hand, a much smaller ratio of Γ_n/Γ_p (~ 1) has been observed for light hypernuclei, where also spectra of fast protons have been analysed. Here, *e.g.*, the results by J.J. Szymanski *et al.* [6] for ${}^{5}_{\Lambda}$He, ${}^{11}_{\Lambda}$B and ${}^{12}_{\Lambda}$C are smaller than 2; this is also in line with the recent measurements of O. Hashimoto *et al.* [10] for ${}^{12}_{\Lambda}$C and ${}^{28}_{\Lambda}$Si.

Table 4. The ratios of decay widths Γ_n/Γ_p for light and heavy hypernuclei obtained from a straightforward detection of fast protons from the nonmesonic decay of the Λ-hyperon.

Hypernucleus or range of masses of hypernuclei	Γ_n/Γ_p	Ref.
$40 < A < 100$	1.5–9.0	[12]
$40 < A < 100$	9.0	[13]
$A \sim 50$	~ 5	[14]
${}^{28}_{\Lambda}$Si	$1.38^{+0.13+0.27}_{-0.11-0.25}$	[10]
${}^{12}_{\Lambda}$C	$1.33^{+1.12}_{-0.81}$	[6]
${}^{12}_{\Lambda}$C	$1.17^{+0.09+0.020}_{-0.08-0.18}$	[10]
${}^{11}_{\Lambda}$B	$1.04^{+0.59}_{-0.48}$	[6]
${}^{5}_{\Lambda}$He	0.93 ± 0.55	[6]

The experimental situation thus appears to create a puzzle; Γ_n/Γ_p is found to be larger than 2 for heavy hypernuclei, whereas it is apparently close to unity for light hypernuclei. Thus, either the analysis of the experiments is biased by some mass-dependent effects, or this ratio is indeed different for light and heavy hypernuclei.

7 Summary

In this work we have summarized the experimental studies of the COSY-13 Collaboration that aimed at measuring the lifetime τ_Λ of the Λ-hyperon in heavy nuclei produced in proton-induced reactions on Au, Bi and U targets employing the recoil shadow method. The lifetimes extracted from the various experiments are all compatible with each other and also with the lifetimes determined by early antiproton annihilation experiments on Bi and U targets from ref. [11], albeit much more accurate. These lifetimes correspond to a broad range in mass and charge of the produced hypernuclei (cf. fig. 3) with a rather narrow dispersion in charge (for fixed A). This mass range is comparable to the mass range of light hypernuclei studied up to now.

Averaging the lifetime τ_Λ over all results from the COSY-13 measurements we obtain

$$\tau_\Lambda = 145 \pm 11 \ \mathrm{ps}\,.$$

This value for the lifetime of heavy hypernuclei is smaller than the results of recent theoretical calculations by W.M. Alberico *et al.* [51] ($\sim$ 188 ps) and D. Jido *et al.* [52] ($\sim$ 165 ps), which have been performed for the full range of masses of hypernuclei, by more than 3 and 2 standard deviations (in the first and the second case, respectively). In the framework of the theoretical model of ref. [30], such a small value for τ_Λ may be explained by a dominance of the neutron-induced over proton-induced decay rates ($R_n/R_p > 2$). This implies that the empirical $\Delta I = 1/2$ isospin rule —found for the vacuum decays of single strange hadrons and assumed to be valid in

the theoretical calculations of W.M. Alberico *et al.* [51] and D. Jido *et al.* [52]— is violated for the in-medium $\Lambda N \to NN$ transition. The latter reactions involve a high momentum transfer, *i.e.* they test the ΛN weak interaction at short distances, where the overlap of the quark wave functions is very large. It is questionable whether these compact "parton configurations" might be described properly in the meson-exchange picture based on effective hadronic Lagrangians. A description with partonic degrees of freedom, which includes automatically $\Delta I = 3/2$ transitions, should be more adequate, but reliable calculations on the partonic level still have to wait for the future. We like to emphasize that such calculations should give an ultimate answer on the validity of the $\Delta I = 1/2$ rule; so far our conclusions are based on a comparison of our data with theoretical models, that all have known deficiencies.

This work has been supported by the DLR International Bureau of the BMBF, Bonn, and the Polish Committee for Scientific Research.

References

1. J. Cohen, Prog. Part. Nucl. Phys. **25**, 139 (1990).
2. E. Oset, A. Ramos, Prog. Part. Nucl. Phys. **41**, 191 (1998).
3. W.M. Alberico, G. Garbarino, Phys. Rep. **369**, 1 (2002).
4. A. Montwill, P. Moriarty, D.H. Davis, T. Pniewski, T. Sobczak, O. Adamovic', U. Krecker, G. Coremans-Bertrand, J. Sacton, Nucl. Phys. A **234**, 413 (1974).
5. R. Grace, P.D. Barnes, R.A. Eisenstein, G.B. Franklin, C. Maher, R. Reider, J. Seydoux, J. Szymanski, W. Wharton, S. Bart, R.E. Chrien, P. Pile, Y. Xu, R. Hackenburg, E. Hungerford, B. Bassaleck, M. Barlett, E.C. Milner, R.L. Stearns, Phys. Rev. Lett. **55**, 1055 (1985).
6. J.J. Szymanski, P.D. Barnes, G.E. Diebold, R.A. Eisenstein, G.B. Franklin, R. Grace, D.W. Hertzog, C.J. Maher, B.P. Quinn, R. Rieder, J. Seydoux, W.R. Wharton, S. Bart, R.E. Chrien, P. Pile, R. Sutter, Y. Xu, R. Hackenburg, E.V. Hungerford, T. Kishimoto, L.G. Tang, B. Bassaleck, R.L. Stearns, Phys. Rev. C **43**, 849 (1991).
7. H. Noumi, S. Ajimura, H. Ejiri, A. Higashi, T. Kishimoto, D.R. Gill, L. Lee, A. Olin, T. Fukuda, O. Hashimoto, Phys. Rev. C **52**, 2936 (1995).
8. H.C. Bhang, S. Ajimura, K. Aoki, T. Hasegawa, O. Hashimoto, H. Hotchi, Y.D. Kim, T. Kishimoto, K. Maeda, H. Noumi, Y. Ohta, K. Omata, H. Outa, H. Park, Y. Sato, M. Sekimoto, T. Shibata, T. Takahashi, M. Youn, Nucl. Phys. A **639**, 269c (1998).
9. Particle Data Group, Eur. Phys. J. C **15**, 1 (2000).
10. O. Hashimoto, S. Ajimura, K. Aoki, H. Bhang, T. Hasegawa, H. Hotchi, Y.D. Kim, T. Kishimoto, K. Maeda, H. Noumi, Y. Ohta, K. Omata, H. Outa, H. Park, Y. Sato, M. Sekimoto, T. Shibata, T. Takahashi, M. Youn, Phys. Rev. Lett. **88**, 042503 (2002).
11. T.A. Armstrong, J.P. Bocquet, G. Ericsson, T. Johansson, T. Krogulski, R.A. Lewis, F. Malek, E. Monnand, J. Mougey, H. Nifenecker, J. Passaneau, P. Perrin, S.M. Polikanov, M. Rey-Campagnolle, C. Ristori, G.A. Smith, G. Tibell, Phys. Rev. C **47**, 1957 (1993).
12. J.P. Lagnaux, J. Lemonne, J. Sacton, E. Fletcher, D. O'Sullivan, T.P. Shah, A. Thompson, P. Allen, Sr.M. Heeran, A. Montwill, J.E. Allen, D.H. Davis, D.A. Garbutt, V.A. Bull, P.V. March, M. Yaseen, T. Pniewski, J. Zakrzewski, Nucl. Phys. **60**, 97 (1964).
13. J. Cuevas, J. Diaz, D.M. Harmsen, W. Just, E. Lohrmann, L. Schink, H. Spitzer, M.W. Teuchner, Nucl. Phys. B **1**, 411 (1967).
14. S.N. Ganguli, M.S. Swami, Proc. Indian Acad. Sci. **67**, 77 (1967).
15. J.F. Donoghue, E. Golowich, B. Holstein, Phys. Rep. **131**, 319 (1986).
16. K. Miura, T. Minanikawa, Prog. Theor. Phys. **38**, 954 (1967).
17. J.C. Pati, C.H. Woo, Phys. Rev. D **3**, 2920 (1971).
18. V.I. Noga, Yu.N. Ranyuk, N.Ya. Rutkevich, P.V. Sorokin, E.V. Sheptulenko, Sov. J. Nucl. Phys **43**, 856 (1986); **46**, 769 (1987).
19. J.P. Bocquet, M. Epherre-Rey-Campagnolle, G. Ericsson, T. Johansson, J. Mougey, H. Nifenecker, P. Perrin, S. Polikanov, C. Ristori, G. Tibell, Phys. Lett. B **182**, 146 (1986); **192**, 312 (1987).
20. K. Hagino, A. Parreño, Phys. Rev. C **63**, 044318 (2001).
21. A. Parreño, A. Ramos, C. Benhold, K. Maltman, Phys. Lett. B **435**, 1 (1998).
22. W.M. Alberico, A. De Pace, M. Ericson, A. Molinari, Phys. Lett. B **256**, 134 (1991).
23. A. Ramos, M.J. Vicente-Vacas, E. Oset, Phys. Rev. C **55**, 735 (1997); arXiV:nucl-th/0206036 v1 (Erratum).
24. J.F. Dubach, G.B. Feldman, B.R. Holstein, L. de la Torre, Ann. Phys. (N.Y.) **249**, 146 (1996).
25. M.J. Savage, R.P. Springer, Phys. Rev. C **53**, 441 (1996); **54**, 2786 (1996) (Erratum).
26. K. Sasaki, T. Inoue, M. Oka, Nucl. Phys. A **669**, 331 (2000); **678**, 455 (2000) (Erratum).
27. C.B. Dover, Few-Body Syst. Suppl. **2**, 14 (1987).
28. J. Cohen, Phys. Rev. C **42**, 2724 (1990).
29. R.A. Schumacher, Nucl. Phys. A **547**, 143c (1992).
30. Z. Rudy, W. Cassing, L. Jarczyk, B. Kamys, P. Kulessa, O.W.B. Schult, A. Strzałkowski, Eur. Phys. J. A **5**, 127 (1999).
31. W.M. Alberico, G. Garbarino, Phys. Lett. B **486**, 362 (2000).
32. P. Kulessa, Z. Rudy, M. Hartmann, K. Pysz, B. Kamys, I. Zychor, H. Ohm, L. Jarczyk, A. Strzałkowski, W. Cassing, H. Hodde, W. Borgs, H.R. Koch, R. Maier, D. Prasuhn, M. Motoba, O.W.B. Schult, Phys. Lett. B **427**, 403 (1998).
33. V. Metag, E. Liukkonen, G. Sletten, O. Glomset, S. Bjornholm, Nucl. Instrum. Methods **114**, 445 (1974).
34. Gy. Wolf, G. Batko, W. Cassing, U. Mosel, K. Niita, M. Schäfer, Nucl. Phys. A **517**, 615 (1990).
35. Gy. Wolf, W. Cassing, U. Mosel, Nucl. Phys. A **552**, 549 (1993).
36. Z. Rudy, W. Cassing, T. Demski, L. Jarczyk, B. Kamys, P. Kulessa, O.W.B. Schult, A. Strzałkowski, Z. Phys. A **351**, 217 (1995).
37. Z. Rudy, W. Cassing, T. Demski, L. Jarczyk, B. Kamys, P. Kulessa, O.W.B. Schult, A. Strzałkowski, Z. Phys. A **354**, 445 (1996).
38. A. Gavron, in *Computational Nuclear Physics*, Vol. **2**, *Nuclear Reactions*, edited by K. Langanke, J.A. Maruhn, S.E. Koonin (Springer Verlag, 1993) p. 108.

39. W. Cassing, V. Metag, U. Mosel, K. Niita, Phys. Rep. **180**, 363 (1990).
40. W. Cassing, E.L. Bratkovskaya, Phys. Rep. **308**, 65 (1999).
41. V.E. Viola, K. Kwiatkowski, M. Walker, Phys. Rev. C **31**, 1550 (1985).
42. Z. Rudy, Report INP No 1811/PH, Cracow 1998 (`http://mezon.if.uj.edu.pl/~kamys/COSY13/zrhab.pdf`).
43. J. Hudis, S. Katcoff, Phys. Rev. C **13**, 1961 (1976).
44. L.A. Vaishnene, L.N. Andronenko, G.G. Kovshevny, A.A. Kotov, G.E. Solyakin, W. Neubert, Z. Phys. A **302**, 143 (1981).
45. B. Kamys, P. Kulessa, H. Ohm, K. Pysz, Z. Rudy, H. Ströher, W. Cassing, Eur. Phys. J. A **11**, 1 (2001).
46. P. Kulessa, W. Cassing, L. Jarczyk, B. Kamys, H. Ohm, K. Pysz, Z. Rudy, H. Ströher, Acta Phys. Pol. B **33**, 603 (2002).
47. Z. Fraenkel, A. Breskin, R. Chechik, S. Wald, R. Abbeg, H.W. Fielding, P. Kitching, S.T. Lam, G.C. Neilson, W.C. Olsen, J. Uegaki, Phys. Rev. C **41**, 1050 (1990).
48. A.A. Kotov *et al.*, Sov. J. Nucl. Phys. **17**, 498 (1974); **19**, 385 (1974).
49. K. Pysz, I. Zychor, T. Hermes, M. Hartmann, H. Ohm, P. Kulessa, W. Borgs, H.R. Koch, R. Maier, D. Prasuhn, Z. Rudy, B. Kamys, W. Cassing, J. Pfeiffer, Y. Uozumi, L. Jarczyk, A. Strzałkowski, O.W.B. Schult, Nucl. Instrum. Methods A **420**, 356 (1999).
50. H. Park, H. Bhang, M. Youn, O. Hashimoto, K. Maeda, Y. Sato, T. Takahashi, K. Aoki, Y.D. Kim, H. Noumi, K. Omata, H. Outa, M. Sekimoto, T. Shibata, T. Hasegawa, H. Hotchi, Y. Ohta, S. Ajimura, T. Kishimoto, Phys. Rev. C **61**, 054004 (2000).
51. W.M. Alberico, A. De Pace, G. Garbarino, A. Ramos, Phys. Rev. C **61**, 044314 (2000).
52. D. Jido, E. Oset, J.E. Palomar Nucl. Phys. A **694**, 525 (2001).